Available online at www.sciencedirect.com
ScienceDirect
C. R. Physique 10 (2009) 775–789
COMPTES RENDUS PHYSIQUE

Complex and biofluids / Fluides complexes et biologiques

Vesicles and red blood cells in flow: From individual dynamics to rheology

Petia M. Vlahovska [a], Thomas Podgorski [b], Chaouqi Misbah [b,*]

[a] *Thayer School of Engineering, Dartmouth College, 8000 Cummings Hall, Hanover, NH 03755, USA*
[b] *Laboratoire de Spectrométrie Physique, UMR 5588, 140, avenue de la Physique, Université Joseph-Fourier, and CNRS, 38402 Saint Martin d'Heres, France*

Available online 18 November 2009

Abstract

The rheology of suspensions of soft particles, such as red blood cells, is a long-standing problem in science and engineering due to the complex interplay between deformable microstructure and the macroscale flow. The major challenge stems from the free-boundary nature of the particle interface. Lipid bilayer membranes that envelop cells and vesicles are particularly complex interfaces because of their unusual mechanics: the molecularly thin membrane is a highly-flexible incompressible fluid sheet. As a result, particles made of closed lipid bilayers (red cells and vesicles) can exhibit richer dynamics than would capsules and drops. We overview the key experimental observations and recent advances in the theoretical modeling of the vesicles and red blood cells in flow. ***To cite this article: P.M. Vlahovska et al., C. R. Physique 10 (2009).***

Résumé

Vésicules et globules rouges sous écoulement : De la dynamique individuelle à la rhéologie. La rhéologie des suspensions de particules molles, telles les globules rouges, constitue depuis longtemps un défi pour les sciences et l'ingénierie à cause du caractère complexe du couplage entre la microstructure et l'écoulement global. La source de la difficulté provient du caractère libre des surfaces des entités en suspension. Les bicouches lipidiques qui composent les membranes des cellules vivantes et des vésicules sont des surfaces particulièrement complexes à cause de leur mécanique inhabituelle : la membrane d'épaisseur moléculaire est très flexible mais en même temps il s'agit d'une surface incompressible. Il en résulte que les particules composées de ces membranes (comme les globules rouges et vésicules) révèlent plus de richesses que ne le font les gouttes ou les capsules. Nous passons en revue les principaux résultats expérimentaux et les progrès théoriques réalisés dans l'étude des vésicules et globules rouges sous écoulement. ***Pour citer cet article : P.M. Vlahovska et al., C. R. Physique 10 (2009).***

Keywords: Lipid membrane; Stokes flow; Blood rheology

Mots-clés : Membrane lipidique ; Écoulement de Stokes ; Rhéologie du sang

* Corresponding author.
E-mail address: cmisbah@ujf-grenoble.fr (C. Misbah).

1631-0705/$ – see front matter
doi:10.1016/j.crhy.2009.10.001

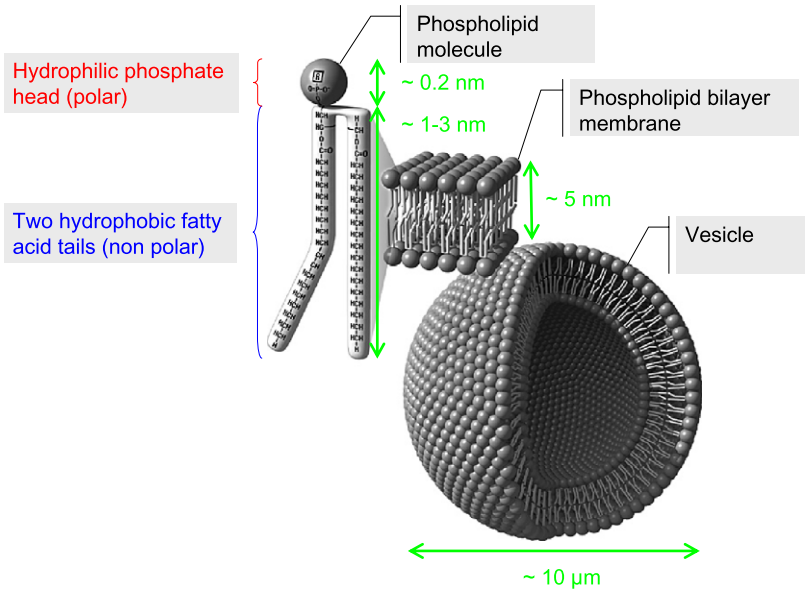

Fig. 1. A cartoon showing a vesicle and the molecular structure of its membrane. Picture taken from the web site of the NASA Astrobiology Institute: *http://astrobiology.nasa.gov/nai/*.

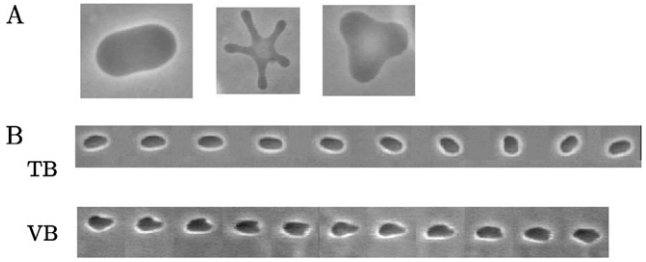

Fig. 2. A. Equilibrium shapes of vesicles [11]. B. Vesicle motions in shear flows: tumbling (TB) and vacillating–breathing (VB) [12].

1. Introduction

Cells and internal cellular organelles are enveloped by membranes composed primarily of lipid bilayers [1–3]. Biomimetic bilayer structures have opened new frontiers in biomedical- and nano-technologies [4]. For instance, bilayer sacs (vesicles) are employed as containers for biochemical reactions as well as for transport and delivery of samples [5,6]; as vectors for targeted drug and gene delivery [7,8]; and as artificial cells for hemoglobin encapsulation and oxygen transport [9].

The biological significance and technological potential of lipid membranes have stimulated an increasing interest in their physics. A giant unilamelar vesicle (see Fig. 1), which is a cell-size membrane envelope, mimics essential characteristics of the red blood cell such as its equilibrium biconcave shape. Thus, vesicles have gained popularity as a model system to study the red blood cell dynamics and membrane biophysics in general [10]. The giant vesicle of large size (10–100 μm) allows the manipulation of individual vesicles and observation of their dynamics in real time with optical microscopy.

Vesicles are fundamentally different from other membrane-bound objects such as polymeric capsules. Vesicles adopt an amazing variety of equilibrium shapes, and exhibit even more complex non-equilibrium dynamics in external flow, see Fig. 2. This rich vesicle behavior stems from the nonlinear coupling of lipid membrane deformation and fluid motion that spans multiple scales. Under stress, lipid membranes store elastic energy in bending [13,14], while polymerized membranes are more likely to be stretched and sheared [15,16]. In addition, the lipid membrane develops a dynamical tension that adjusts itself to the forces exerted on the membrane in order to keep the local area constant.

Finally, lipid membranes are extremely soft and can be easily bent by thermal noise on length scales smaller than $\sqrt{\kappa/\sigma}$, where κ is the bending rigidity and σ is the tension of the membrane. For vesicles at rest, this critical length is comparable to the vesicle radius and the vesicle shape "flickers".

In this review we discuss the current understanding and open questions regarding the dynamics of an isolated vesicle and the collective behavior of many vesicles in suspension. Detailed knowledge of this problem will serve as a solid basis for understanding the red cell dynamics and blood rheology.

2. Background

A pure lipid membrane consists of two sheets of lipid molecules. Lipid bilayers spontaneously close to avoid exposure of their hydrophobic core to water, and form vesicles. The physical properties of lipid bilayers and vesicle configurations are surveyed in the classical reviews by Seifert [14] and Bloom et al. [17], and more recently by Dimova et al. [18]. The bilayer thickness is 5 nm, about 1/1000 of the cell radius. Due to the large separation of length scales, the membrane can be regarded as a two-dimensional surface embedded in a three-dimensional space, and continuum mechanics description applies [19]. In what follows we shall describe first the basic features of membrane forces, equilibrium shapes at rest, and then introduce an external flow in order to study the dynamics and rheology.

2.1. Forces exerted by a bilayer membrane on a surrounding fluid

The bilayer thickness imparts resistance to bending. Within the framework of the spontaneous curvature model [14], the bending resistance gives rise to a surface force density

$$\tau^{\kappa} = -\kappa\big[(2H - C_0)\big(2H^2 - 2K + C_0 H\big) + 2\nabla_s^2 H\big]\mathbf{n} \tag{1}$$

where κ is the bending modulus, H is the mean curvature, K is the Gaussian curvature, C_0 is the bilayer spontaneous curvature (intrinsic curvature due to asymmetry in packing density of the lipid molecule's head and tail [20]), and $\mathbf{n}$ is the normal vector. ∇_s is the surface gradient (gradient along the membrane) and ∇_s^2 refers to the surface Laplacian (also called the Laplace–Beltrami operator). Phospholipid membranes are remarkably soft, because the energy required for bending is comparable to the thermal energy $k_B T$; the bending modulus is $\kappa \sim 20 k_B T$ [18].

The membrane leaflets represent an assembly of fixed number of lipids. The energy cost of increasing the area per lipid is very high as evidenced by the large area expansion modulus $K_a \sim 0.2$ N/m [18]. Accordingly, the membrane can be regarded as a two-dimensional incompressible material (under moderate stresses). A membrane element only deforms, but cannot change its local area. That is to say, we need to introduce a local Lagrange multiplier σ (i.e. a multiplier that depends on position) that preserves area. From physical point of view, under stress, the membrane develops tension, which adapts itself to the forces exerted on the membrane in order to keep the local and total area constant. Hence, the tension may become non-uniform along the interface and varies with forcing. The membrane tension gives rise to surface force density

$$\tau^{\sigma} = 2\sigma H\mathbf{n} - \nabla_s \sigma \tag{2}$$

where σ denotes the local membrane tension. The first term is normal (and is akin to the Laplace force), while the second one is tangential.

At physiological temperatures, lipid molecules are free to move within the monolayer, and therefore, in contrast to solid-like polymerized membranes, the lipid bilayer membrane is fluid with a zero shear-elastic modulus [18]. The two-dimensional membrane viscosity of lipid bilayers is of about $\eta_{\mathrm{mm}} \sim 10^{-9}$ N s/m. If d denotes the membrane thickness (of order of 5 nm), then the equivalent three-dimensional viscosity is of about $\eta_{\mathrm{mm}}^{3D} \sim \eta_{\mathrm{mm}}/d \sim 0.2$ N s/m^2, which is much larger than the water viscosity, $\eta = 10^{-3}$ N s/m^2. However, since the hydrodynamic dissipation inside the membrane extends over the thickness d, while that in the surrounding fluid over a distance of the order of the vesicle size R_0, membrane dissipation prevails only if $(\eta/\eta_{\mathrm{mm}}^{3D})R_0 < d$. This entails that membrane dissipation would be relevant only at quite small scales, below 1 μm. Since we are interested in the so-called giant vesicles the membrane dissipation is quite negligible.

In the red blood cell (RBC), a key component of the membrane is a protein scaffold attached to the lipid bilayer (Fig. 3). The polymer network endows the RBC membrane with resistance to shearing. As a result, RBCs are often modeled as capsules with elastic membrane stresses described by Skalak's constitutive law (see detailed discussion in [21]).

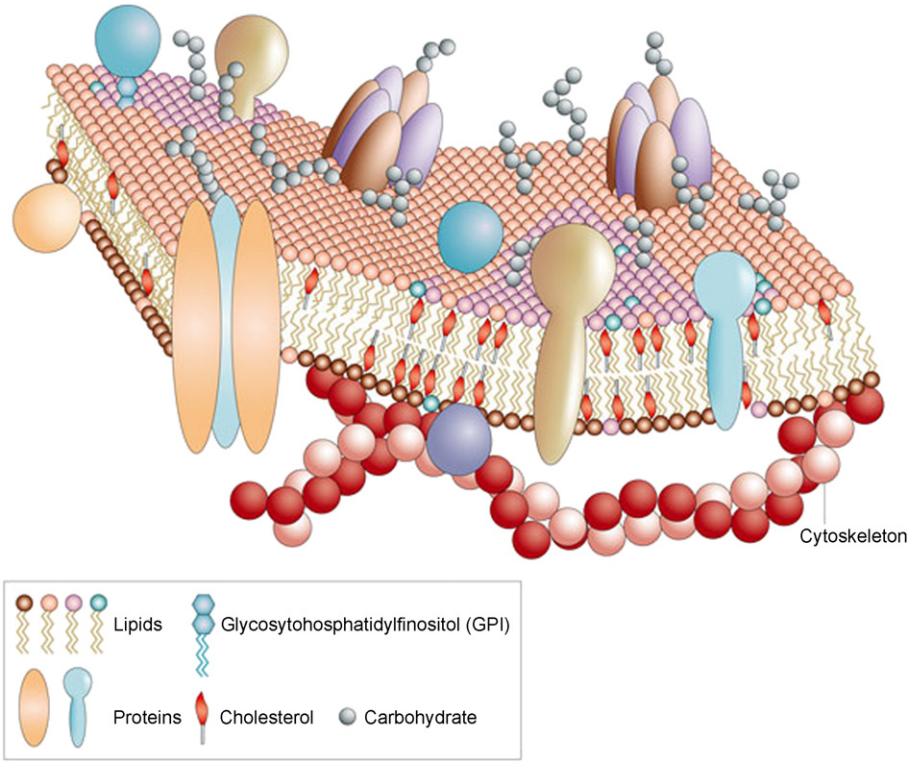

Fig. 3. Cartoon presenting the components of which a red blood cell membrane is made. Besides the bilayer structure (made of molecules having a head and two tails), the membrane is made of many other species, like the cytoskeleton filaments.

2.2. *Equilibrium shapes of vesicles*

At equilibrium, the membrane tension is uniform. The fluids on both sides exert only hydrostatic pressure, which acts normal to the interface. Hence, the only tangential component of the membrane forces (Eq. (2)), $\nabla_s \sigma$, is zero which implies uniformity of σ. Equilibrium vesicle shapes correspond to solutions of the generalized Laplace's equation [22–25]

$$p^{\text{in}} - p^{\text{ex}} = 2\sigma H - \kappa\left[4H^3 - 4KH + 2\nabla_s^2 H\right] \tag{3}$$

where, for simplicity, we have set the spontaneous curvature to zero. It balances hydrostatic pressure, bending (Eq. (1)) and capillary tractions (Eq. (2)). Like the tension σ, the pressure p can also be viewed as a Lagrange multiplier that enforces constant enclosed volume. The membrane area is constant because the number of molecules in the bilayer is fixed. The enclosed volume is also constant, because the membrane is impermeable to ions and osmotic pressure resists changes in volume. Equilibrium vesicle shapes have been exhaustively studied and vesicle topology has been mapped as a function of the spontaneous curvature and excess area Δ, which is the difference between the vesicle area and the area of an equivalent volume sphere [26,14,20]

$$\Delta = \frac{A}{R_0^2} - 4\pi, \quad R_0 = \left(\frac{3V}{4\pi}\right)^{1/3} \tag{4}$$

$\Delta = 0$ for a sphere, and $\Delta > 0$ otherwise. For red blood cells $\Delta \simeq 5$. The characteristic red blood cell shape of a biconcave disc corresponds to a minimum of the bending energy at excess area about 5 [14].

There are several extensions of the basic curvature model defined by Eq. (1). The bilayer couple and the area-difference elasticity (ADE) models [14,20] were introduced in order to account for more complex shapes such as the starfish one, see Fig. 2.A. Note that the equilibrium solutions correspond in reality to an average shape, since the equilibrium tension of vesicles can be very low, $\sigma_0 \sim 10^{-6}$ N/m, and the energy cost for bending is low $\kappa \sim k_B T$, so that thermally induced membrane undulations make the surface "flicker" [27,28].

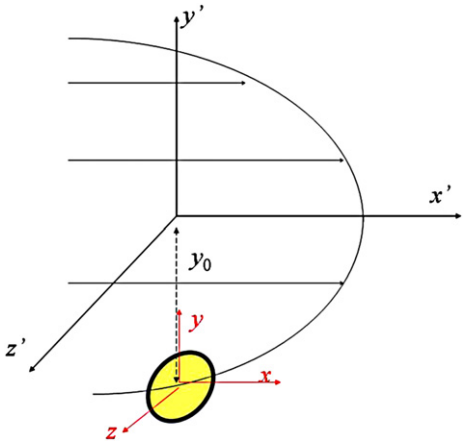

Fig. 4. Sketch of the streamlines of Poiseuille flow. A cell is placed off-center at a distance y_0.

2.3. *Fluid motion and fluid–membrane coupling*

At the length scale of a micron-size vesicle, water is effectively very viscous and low-Reynolds number (creeping flow) conditions prevail. Forces are locally balanced and vesicle motion is described by the Stokes equations

$$\nabla \cdot \mathbf{T} = 0, \qquad \nabla \cdot \mathbf{v} = 0 \tag{5}$$

where $\mathbf{T}$ is the bulk hydrodynamic stress

$$\mathbf{T} = -p\mathbf{I} + \eta\big(\nabla\mathbf{v} + (\nabla\mathbf{v})^{\dagger}\big) \tag{6}$$

p is the pressure, η is the fluid viscosity, $\mathbf{I}$ denotes the unit tensor and the superscript † denotes transpose, $\mathbf{v}$ is the velocity. Far away from the vesicle, the flow field tends to the unperturbed external flow $\mathbf{v}^{\text{ex}} \to \mathbf{v}^{\infty}$. The surrounding fluids exert tractions on the membrane that are balanced by membrane forces

$$\mathbf{n} \cdot \big(\mathbf{T}^{\text{ex}} - \mathbf{T}^{\text{in}}\big) = \tau^{\kappa} + \tau^{\sigma} + \tau^{\text{el}} \tag{7}$$

Surface forces due to the lipid bilayer are given by Eqs. (1) and (2). τ^{el} are elastic tractions due to the spectrin network; these are evaluated using appropriate constitutive laws [21,15]. For fluid vesicle at rest, Eq. (7) reduces to the Euler–Lagrange (generalized Laplace) equation (Eq. (3)).

3. Dynamics of an isolated vesicle and red blood cell in flow

Equilibrium vesicle and red blood cell (RBC) dynamics, i.e., membrane fluctuations around locally stable shape, is a well researched topic in statistical physics [28,29]. Non-equilibrium dynamics is the more challenging and far less explored regime. The past several years have marked an increasing interest in the motions and deformation of vesicles and RBCs induced by external fields such as fluid flow.

The focus of this review is on flows relevant to the microcirculation. Let us consider the pressure-driven flow in a capillary (Poiseuille flow), see Fig. 4. In the lab frame, an axisymmetric Poiseuille flow in the absence of cells or vesicles is described by $\mathbf{v}^{\infty} = [U_c - \alpha(y'^2 + z'^2)]\hat{\mathbf{x}}'$, where α is a measure of the curvature of the flow profile and U_c is flow velocity at the centerline. If a cell is placed off-center, e.g., at position $(x_0, y_0, 0)$, it "sees" flow which is a combination of linear shear and quadratic component

$$\mathbf{v}^{\infty} = \big[\dot{\gamma}\, y + \alpha\big(y^2 + z^2\big)\big]\hat{\mathbf{x}} - \mathbf{U}_{\text{mig}} \tag{8}$$

where $\dot{\gamma} = 2\alpha y_0$ is the local shear rate, and the migration velocity $\mathbf{U}_{\text{mig}}$ is the difference between the velocities of the cell and the undisturbed flow at the cell center. A rigid sphere lags the flow, $\mathbf{U}_{\text{mig}} = (2\alpha/3)U_c\hat{\mathbf{x}}$, a result that follows from Faxen's law [30]. The questions are: *Do vesicles and RBC deform in flow, and how does the deformation affect their motions*?

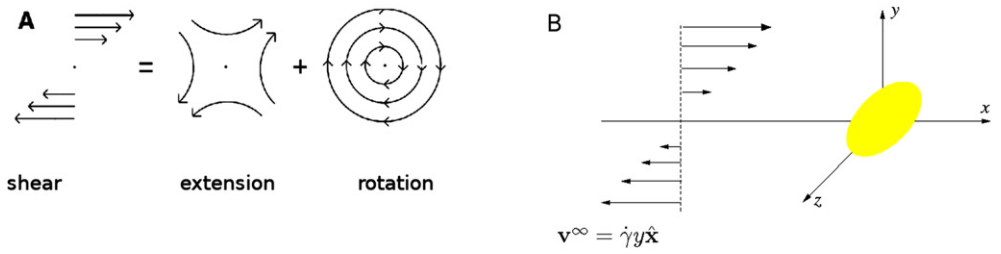

Fig. 5. A. Sketch of the streamlines of a linear shear flow. The flow is a superposition of pure straining and rigid body rotation. B. A soft particle deforms to an ellipsoid in a simple shear flow.

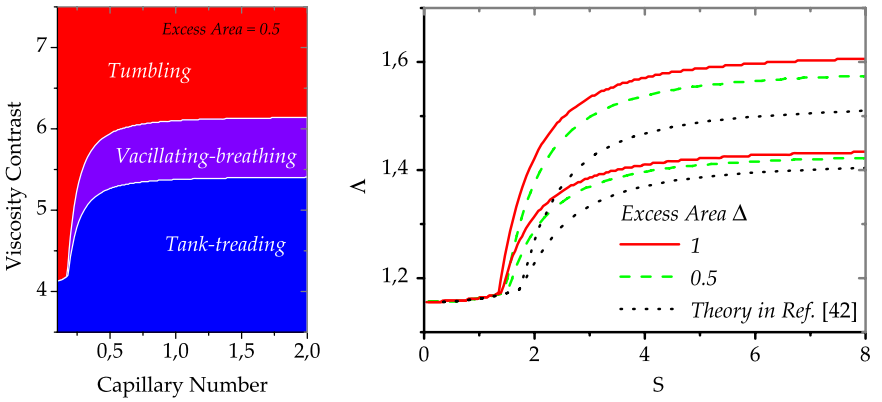

Fig. 6. (Color on line.) Left: A phase diagram representing the three regimes: TT, VB and TB in the (λ–Ca) plane. Right: Phase diagram in the plane S–Λ, with $S = c_1 Ca/\Delta$, $\Lambda = c_2\sqrt{\Delta}(32 + 23\lambda)$, where $c_1 = 14\pi/\sqrt{27}$, $c_2 = \sqrt{3/10\pi}/24$. This diagram shows that the boundaries between the three regimes are sensitive to Δ, unlike the theory in Ref. [42]. These figures are extracted from Ref. [43].

If the vesicle or RBC is very far away from the centerline, the linear shear dominates. Therefore, first we consider linear flows and after that discuss effects from flow curvature.

3.1. Linear flows

3.1.1. Experiments

Vesicles and red blood cells in unbounded steady shear flow (see Fig. 5) have been observed to exhibit at least three different types of dynamics [31–33,12,34,35]: (1) *tank-treading* (TT), where the vesicle deforms into a prolate ellipsoid inclined at a stationary angle with respect to the flow direction; (2) *tumbling* (TB), where the vesicle undergoes a periodic flipping motion; and (3) *vacillating breathing* (VB) [36], where the vesicle long axis makes oscillations about the flow direction and the shape exhibits breathing. This type of motion has been l alternatively called *trembling* [33] and *swinging* [38].

The details of the dynamics depend on three parameters: the vesicle's excess area, which governs its equilibrium shape, the ratio between internal and external viscosities λ, and the dimensionless shear rate or capillary number, $Ca = \eta\dot{\gamma} R_0^3/\kappa$. If the shape is fixed as assumed by Keller and Skalak [37] only TT and TB exist. Allowing the shape to freely evolve has led to the discovery of a new type of motion, namely VB [36]. This mode was initially (in the very first step of the theory) [36,39] predicted to coexist with TB. Experiments have reported that VB exists for intermediate λ or capillary number [33]. Another measurable effect of increasing the capillary number on tumbling vesicles is a decrease of the tumbling frequency when approaching the transition to VB [12,40]. There is a consensus from theoretical studies that the phase diagram of the three regime (TT, VB and TB) has the shape shown in Fig. 6 (left panel).

Recently Deschamps et al. [35] made extensive measurements of vesicle dynamics by varying all parameters and recovered experimentally a phase diagram in good qualitative agreement with recent theories for weakly deflated vesicles [41,42], see Fig. 7. The work by Lebedev et al. [42] reported that among the three independent parameters

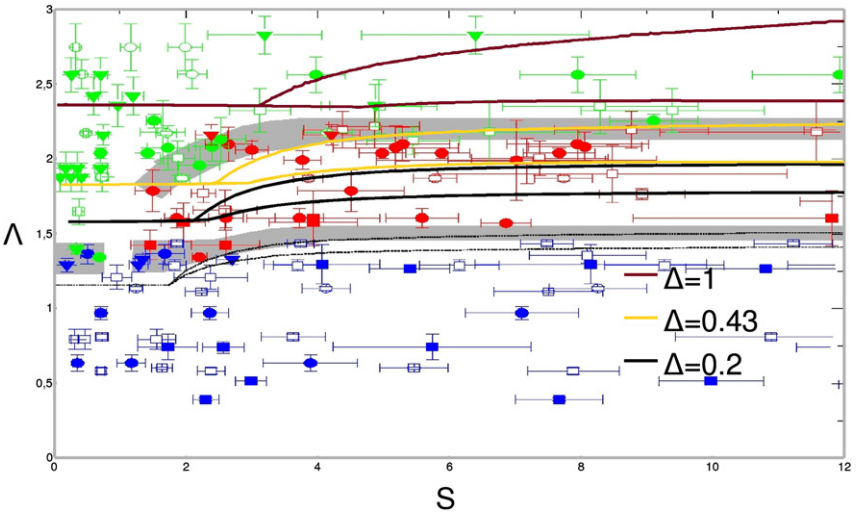

Fig. 7. Phase diagram of the vesicle dynamics in shear flow [35]. Blue symbols denote TT motion, red – VB, and green – TB. The dotted lines are the theory of Ref. [42], while the full lines are the theory of Ref. [44].

Ca, λ and Δ only two are relevant; these are denoted S and Λ and are function of the above three parameters; their definition is given in the caption of Fig. 6. The study of Danker et al. [41] has shown (due to their consistent perturbation theory) that three parameters survive (which can be chosen to be *Ca*, λ and Δ, or equivalently S, Λ and Δ as used in Fig. 6). More recently, Kaoui et al. [43] have discussed in details the issue regarding the relevance of the three parameters. A result which has emerged there is that by keeping S and Λ constant, and varying the third parameter (which may be taken to be Δ) the boundaries of the phase diagram of Fig. 6 change significantly (Fig. 6, right panel), in contrast to Refs. [42,35]. Data of Fig. 7 obtained for different values of Δ, as extracted from Ref. [35], were mixed together, since the authors assume the so-called similarity (in a sense that only S and Λ are relevant) property put forward in Ref. [42]. Kaoui et al. [43] have further shown that, beside the location of the boundaries in the phase diagram, other quantities (like the amplitude of oscillation of the long axis of the VB mode) are extremely sensitive to the third parameter Δ (when S and Λ are kept constant).

Finally, it must be mentioned that results from analytical theories [41,42], while they agree on the qualitative shape of the phase diagram (Fig. 6), they both found a significant shift towards significantly lower values of λ (or Λ) as compared to experiments (Fig. 7; see dotted lines in that figure which have a quite large discrepancy as compared with experiments). This problem has been recently cured both analytically [44] and numerically [45]. This is attributed to the fact that in previous analytical theories only the second-order spherical harmonic in the vesicle shape equation has been retained, while it turns out that the fourth-order harmonic contribution has an important impact [44].

Experiments at very low shear rates (namely when the ratio of shear stress to thermal energy $\zeta = \dot{\gamma}\eta_{\text{out}}R^3\Delta^{1/2}/kT$ is not too large [25,32]) show a significant influence of the thermal fluctuations on the shape and orientation of vesicles. This is especially visible on the orientation in the tank-treading regime [32] and on vesicle shape in the VB mode [33,12,35] where the membrane is quite flaccid in the contraction phase of the vacillating–breathing (or trembling) mode. However, by performing ensemble average, they showed [32] that the average behavior is well described by the noise-free models.

3.1.2. Analytical theory

Analytical solutions can be found in the limit of a nearly-spherical shape [25,46,36,39,41,47,42]. The departure of the vesicle shape from a sphere is characterized by the excess area (Eq. (4)), thus the theory is valid for $\Delta \ll 1$. Neglecting membrane thermal undulations, at leading order the shape evolution is described by the inclination angle ψ and the length of the major axis R [36]

$$\frac{\partial\psi}{\partial t} = -\frac{1}{2} + \frac{h}{2R(t)}\cos\bigl[2\psi(t)\bigr] \tag{9}$$

$$\frac{\partial R}{\partial t} = h\left(1 - 4\frac{R(t)^2}{\Delta}\right)\sin\bigl[2\psi(t)\bigr] \tag{10}$$

where $h = 4\sqrt{30\pi}/(23\lambda + 32)$ and $\lambda = \eta_i/\eta_o$ is the ratio of viscosities of the inner and outer fluids. If deformation along the vorticity (z) axis is suppressed, $R(t) = \text{const}$ and Eq. (9) reduces to the Keller–Skalak phenomenological model, which describes the dynamics of a tank-treading ellipsoid with fixed shape [37].

The evolution equations show that the vesicle dynamics is remarkably different from capsules and drops. First, the equations are *nonlinear*, unlike drops and capsules, whose response to external flow is linear at leading order. Second, the dynamics is *independent of the elastic properties* of the interface; the capillary number, *Ca*, scales out of the equations. This peculiar behavior is a consequence of the area constraint: at leading order, vesicle motion is governed by the tension that arises from the membrane incompressibility. The tension is not a material property of the membrane, but a dynamical variable that ensures that shape deformation exactly satisfies the area constraint. The tension depends on the flow-induced deformation and increases with the flow strength, *Ca*; in shear flow $\sigma_0(t) \sim CaR(t)\sin 2\psi(t)$.

The set of coupled nonlinear equations has a stable fixed point (corresponding to TT) below λ_c; the TT–TB transition occurs at a critical viscosity ratio

$$\lambda_c = -\frac{32}{23} + \frac{120}{23}\sqrt{\frac{2\pi}{15\Delta}} \tag{11}$$

The theory [36,39] agrees qualitatively well with experimental data [115,117]. A rheological constitutive law has been derived [114] that should serve as a first step from microscopic considerations towards blood rheology.

The perturbation analysis has been extended to include membrane bending elasticity [41,42] and thermal fluctuations [25,48]. A higher-order theory captures the effects due to bending elasticity. The phase diagram of vesicle motions agrees qualitatively well with experiments [35]. Thermal fluctuations are shown to induce intermittent tumbling and modify the tank-treading to tumbling transition [48,49]. Furthermore, effects of time-dependent external flow have been investigated, albeit to a limited extent. Oscillatory shear reduces membrane fluctuations, probably due to increase in the membrane tension [50]. Upon reversal of the flow direction, a vesicle displays transient membrane wrinkles [51]. The small-scale undulations of the membrane have been attributed to the appearance of negative tension [52], which enhances the thermally induced fluctuations of the membrane.

3.1.3. Numerical simulations

The dynamic behavior of vesicles with large excess area can be explored only by means of numerical simulations. Numerical simulations of lipid membranes are abundant [19,53–55], but here we focus only on studies that address vesicles in external flows. The computational approaches fall into three categories depending on how the fluid and the membrane are modeled: continuum, e.g., the Boundary Integral Method (BIM) [56–59], particle-based, e.g., dissipative particle dynamics [60,61], or hybrid such as multi-particle collision dynamics [62,49,63,38,64,65]. The continuum models apply to cell-sized vesicles. The BIM is arguably the most accurate but very computationally expensive technique. Alternative approaches are the phase-field method [66–68] (also successfully applied to compute equilibrium vesicle shapes [69]) and the finite element method [70,71], which thus far has been employed only to study equilibrium shapes. Numerical modeling of vesicles in flow is still at an early stage and numerical predictions not always agree. For example, Noguchi and Gompper [49] report stationary tank-treading discocyte shape, while Kraus et al. [56] find only prolate one. More extensive simulations are needed to establish the correct vesicle shape variations with the flow.

In the case of RBCs, most classic studies have focused on the solid-elastic properties of the RBC membrane [72,22] and neglected the characteristics due to the lipid bilayer, such as bending resistance [73] and even incompressibility [74], with few exceptions [75–77].

3.1.4. Red blood cells: New features

The phase diagram of red blood cells is richer compared to vesicles, due to the elasticity of the spectrin network. In addition to TT, VB, and TB, RBC's display a new motion: tank-treading accompanied by small oscillations in the inclination angle, dubbed *swinging* (SW) [78]. The denomination SW is also used to designate the VB mode by other authors, since both modes have similar visual characteristics. A main difference between vesicles and RBC's is that

for small viscosity ratios vesicle show TT while RBC's perform a tumbling motion at low shear rates, then switch to swinging at intermediate shear rates, and tank-tread at high shear rates [79,78,34]. At high shear rates, though, the dynamics is similar to vesicles, with TT at low viscosity ratio, VB at intermediate λ and TB at high λ.

The recently reported swinging motion [78] has also been observed with capsules [80] and drops covered with adsorbed protein layer [81]. Hence, swinging dynamics has been credited to the shear elasticity of the encapsulating membrane and the non-spherical rest shape of the RBC. Phenomenological models [78,82] based on the Keller–Skalak theory [37] qualitatively capture the physics of the phenomenon. In these models, at low shear rates, RBCs tumble because elastic tensions immobilize the interface, and at higher shear rates RBCs tank-tread. The swinging occurs because owing to the non-spherical reference shape, a membrane element stores elastic energy. During one TT period, the element passes twice through its unstressed position where it releases elastic energy. However, a quantitative description of the swinging phenomenon is lacking. Notably, Skotheim and Secomb [82] predicted intermittent behavior, for which no conclusive evidence was found in the numerical simulations [83–85]. The model put forward by Abkarian et al. [78] agreed with the experimental data only if the shear elastic modulus of the membrane was unrealistically large (by an order of magnitude). A rigorous analytical model that accounts for membrane incompressibility and shape deformation is needed [86]. The topic of red blood cells in a channel is discussed at length in Ref. [87].

3.1.5. Wall-induced migration

In his pioneering studies on blood flow in capillaries, Poiseuille observed that the radial distribution of cells becomes inhomogeneous [88]. The existence of a cell-depleted region near the walls accounts for the Fahraeus–Lindqvist effect, which is the decrease of the apparent blood viscosity in small blood vessels with diameter < 500 μm [89]. Cell motion transverse to the flow direction can be driven by wall-repulsion or shear-gradients, which are discussed in Section 3.2.2.

A classic result in microhydrodynamics is that lateral migration of a neutrally-buoyant, non-deformable spherical particle is prohibited in the creeping-flow limit. This conclusion follows from the linearity of the Stokes equation and boundary conditions, and the symmetry of the problem under flow-reversal [90,30]. However, a cross-stream drift may occur if the symmetry is lost, e.g., by particle deformation in a shear gradient or in the presence of a wall [91].

It has been observed experimentally [92–95] that a vesicle in tank-treading motion in a shear flow near a wall experiences a lift force which pushes it away from that wall. A considerable theoretical interest has been devoted to this problem [96–101]. The hydrodynamic repulsion between the vesicle and the wall can be analyzed using the method of images [102]: the boundary conditions at the wall can be satisfied by placing a vesicle hydrodynamic image on the opposite side. The flow field due to the image pushes the "real" vesicle away from the wall. A vesicle well separated from the wall, $d \gg R_0$, where d is the distance to the wall and R_0 is the vesicle radius, moves away from the boundary with velocity [39]

$$\mathbf{U}_{\mathrm{mig}} = \hat{\mathbf{y}}\dot{\gamma} R_0^3 \frac{1}{d^2}\frac{3}{32}\frac{\Delta(23\lambda+32)}{8\pi}\left[-1+\frac{1920\pi}{\Delta(23\lambda+32)^2}\right]^{\frac{1}{2}} \tag{12}$$

A similar scaling was found by Olla [99–101]. The lift force is simply $F_{\mathrm{lift}} = 6\pi\eta R_0 U_{\mathrm{mig}}$.

The first experimental studies on the lift from a wall dealt with the initial stages of the unbinding of a vesicle adhering to the wall [92,93]. Abkarian et al. investigated the lift force on a vesicle detaching from a wall under shear flow and under gravity [93,94]. In this scenario, the vesicle moves until the lift force is balanced by the vesicle weight. The reported dependence of the migration velocity on the distance from the wall was $1/d$, not $1/d^2$ as expected from Eq. (12). This discrepancy can be attributed to the fact that the vesicle remains rather close to the wall. Indeed, Callens et al. [95] performed experiments in microgravity conditions, where only the lift force is present, and found that at distances larger compared to vesicle size, the lift velocity is quantitatively well described by Olla's model [99–101], which is also consistent with Eq. (12) cited above. So far, however, the quantitative influence of the viscosity ratio has not been studied experimentally, although it seems clear that an increase of the viscosity ratio should decrease the lift velocity due to a smaller inclination angle of the vesicle, and therefore a smaller fore-aft asymmetry.

The near-contact motion of the vesicle (very close to the wall) has been studied only to a limited extent. In this case, shape deformation plays a prominent role. Accordingly, the migration velocity (and lift force) varies quadratically with the shear-rate $\dot{\gamma}$ as confirmed numerically [96]. However, studies on the thin liquid dynamics between the membrane and the wall are non-existent.

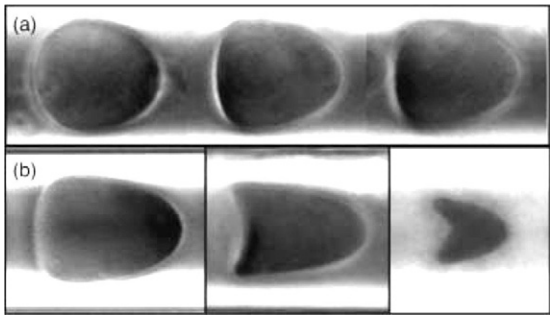

Fig. 8. Shapes of vesicles in capillaries (from [107]). (a) Deformation of one vesicle ($R_0 = 20.2$ μm, $\Delta = 0.14$, $\lambda = 0.71$) at increasing velocities ($U = 36$, 292, 491 μm/s). (b) Other examples of shapes (corresponding parameters are $R_0 = 20.9$, 18.8 and 8.7 μm; $\Delta = 0.46$, 1.7 and 2; $\lambda = 0.80$, 0.67 and 0.40; $U = 219$, 541 and 505 μm/s and $a = 0.15$, 0.29 and 0.50). Scale: picture height is about 50 μm.

3.2. Capillary flows

3.2.1. Vesicles and red blood cells in narrow channels

In capillaries with diameter comparable to the cell size, vesicles and red blood cells align with the flow axis and adopt a bullet or parachute shape depending on their excess area and speed, see Fig. 8. Due to the axial symmetry, the tension gradients immobilize the interface so the vesicle moves as a solid body. In channels which are larger than vesicle size, very deflated objects (such as red blood cells) can exhibit a slipper shape which is not centered in the channel in the steady state [103–105,34]. Very recently [106], it has been shown that a vesicle can also deform into a slipper and a theoretical explanation of this phenomenon has been given. This finding underscores the generic character of the slipper phenomenon. The ratio of vesicle or cell velocity to the mean flow velocity (sometimes known as mobility) is usually larger than 1 and increases when vesicle size decreases [107,108].

3.2.2. Curvature-induced migration

Recently, the cross-stream migration of vesicles in a parabolic velocity profile was investigated theoretically [109] and numerically [58] in an unbounded flow, and experimentally in microchannels where interactions with walls cannot be neglected [110]. The results have shown that vesicles always migrate towards the flow centerline, unlike surfactant-free drops, for which the migration direction depends on the viscosity ratio [111,91]. In general, vesicles are governed by the non-uniform tension and the migration is in direction which minimizes the asymmetry in the tension distribution.

A detailed analytical calculation [109] has identified the ratio between the inner and outer fluid viscosities λ as the main controlling parameter and it has confirmed that the membrane bending and shear elasticity are of less importance. At low λ, the vesicle deforms into a tank-treading shape, which is an ellipsoid if the vesicle is far-away from the flow centerline. Above a critical λ, the vesicle tumbles and cross-stream migration is suppressed. The theory predicts a surprising coexistence of two types of shapes at the centerline, a bullet-like and a parachute-like shape. Similar shapes have been recently observed in numerical simulations [64]. Fig. 9 shows that as the vesicle moves towards the centerline, its shape deforms more and more until it becomes a parachute (or assumes another shape, namely bullet-like) when the centerline is reached.

Interestingly, in the case of an unbounded parabolic velocity profile, when the vesicle is far-away from the centerline its cross-stream migration velocity becomes independent of the local shear rate and depends only on the gradient of shear rate, which is uniform in the flow.

In experiments where both the curvature of the flow field and the walls are present [110], the migration velocity scales like $R_0^{\delta+1}\dot{\gamma}(d)/d^{\delta}$, where R_0 is the vesicle radius, $\dot{\gamma}(d)$ the local shear rate, with an exponent $\delta \simeq 1$. The same scaling seems to hold for 2D boundary integral method simulations of a vesicle near a wall in a parabolic velocity profile [110]. The amplitude of the migration velocity depends strongly on the viscosity ratio λ and the excess area Δ. For low viscosity ratios, for which only the tank-treading mode is seen in the range of studied excess areas, the migration velocity increases as the vesicle gets more deflated. The migration velocity is a decreasing function of λ (for a given value of Δ) and at high λ, it exhibits a non-monotonic behavior when varying Δ: starting from a sphere

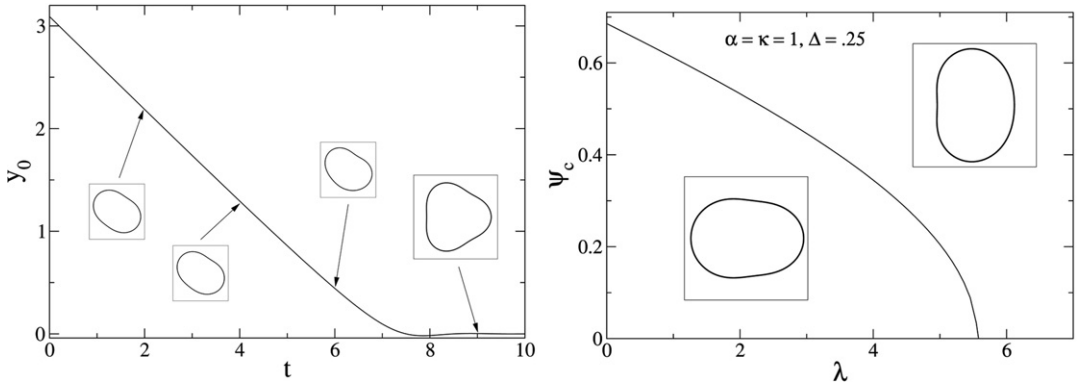

Fig. 9. Left: Evolution of the vertical position of the vesicle as a function of time. Some snapshots of the vesicle shape along the trajectory are shown as insets. Right: Shapes at the centerline [109].

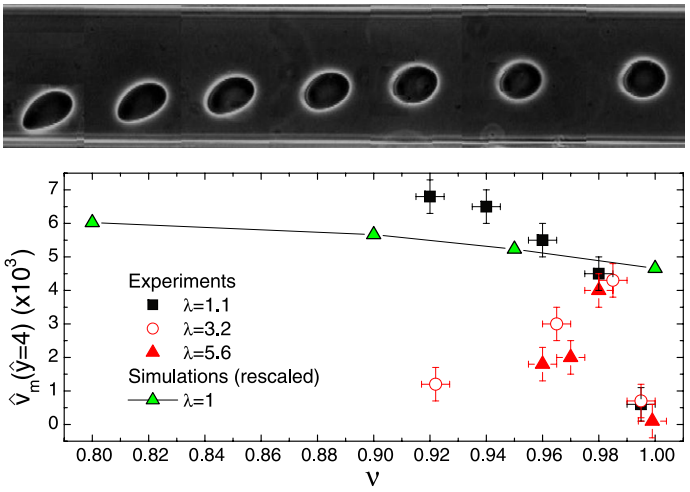

Fig. 10. Top: Migration of a vesicle towards the center of a microchannel (vesicle radius $R \simeq 9.5$ μm, channel width 70 μm, viscosity ratio $\lambda = 1.1$ and excess area $\Delta = 0.58$). Bottom: Migration velocity at a distance $y/R_0 = 4$ vs. reduced volume for different viscosity ratios; $v = (1 + \Delta/4\pi)^{(-3/2)}$. Figures from [110].

($\Delta = 0$), the migration velocity increases when deflating the vesicle, then reaches a maximum and decreases back to a very low value at Δ close to the transition to tumbling, see Fig. 10.

Flow through capillaries with variable cross-section has also been studied. Experiments have shown that a constriction in the flow dramatically widens the cell-free layer downstream [112]. This effect has been qualitatively interpreted as a result of cell migration due to hydrodynamic repulsion by the wall, however rigorous description of the phenomenon is lacking.

4. Rheology of vesicle suspensions

A suspension of particles can be described as a continuum at length scales large compared to the size of the constituent particles. Adding particles typically increases the fluid viscosity. In dilute suspensions, where particles are too far from each other to hydrodynamically interact, the increase in effective stress is just a sum of the stress contributions of the individual particles [102,113].

The asymptotic analysis for a nearly-spherical vesicle predicts a shear-rate-independent suspension rheology at leading order. The shear viscosity decreases with viscosity ratio and attains a minimum value at λ_c, corresponding

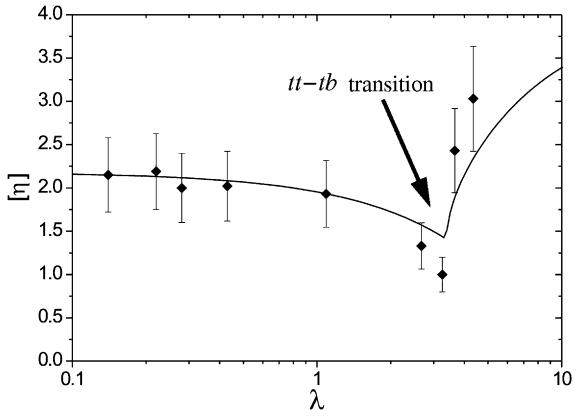

Fig. 11. Viscosity of a RBC suspension $(\eta_{\text{eff}} - \eta_0)/\eta_0\varphi$ versus viscosity ratio λ [115]. The volume fraction is in the range $3\% < \varphi < 12\%$. The solid line shows the analytical result calculated from Eq. (13). Minimum viscosity occurs at the *tt–tb* transition.

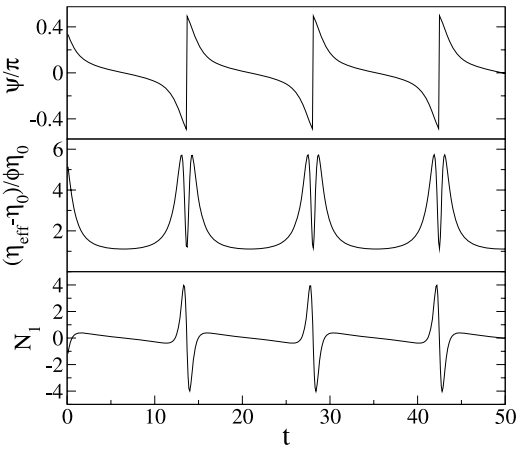

Fig. 12. The time-dependent orientation angle (upper panel), the time-dependent viscosity (middle panel) and the first normal stress difference (lower panel) in the tumbling regime [114].

to the TT–TB transition [36,39,114], in agreement with experiments [115] as seen in Fig. 11. For vesicles in the *tank-treading* regime, the difference between the suspension viscosity, η_{eff}, and solvent viscosity, η_0 is [36]

$$\frac{(\eta_{\text{eff}} - \eta_0)}{\eta_0\varphi} = \frac{5}{2} - \Delta\frac{(23\lambda + 32)}{16\pi} \tag{13}$$

where φ is the vesicle volume fraction. In the limit of a spherical particle, $\Delta = 0$, and since a sphere with fixed area and volume in shear flow undergoes only a rigid body rotation, the Einstein's result for a suspension of rigid spheres is recovered. The effective viscosity decreases with the increase of the excess area because the deformable vesicles elongate and thus offer less resistance to the flow. In the case of a *tumbling* vesicle, the suspension effective stress becomes time-dependent and periodic [114], see Fig. 12. The viscosity shows a nontrivial dynamical behavior. It exhibits a minimum at $\psi = 0$, which is intuitive, since the vesicle is aligned with the flow. Surprisingly, another minimum is found at $\psi = \pi/2$, presumably due to the fact that at the same time the shape elongation is minimal. Interestingly, while the experimental data of Vitkova et al. [115] agree with the theory [114,116], Kantsler et al. [117] found that at low λ the effective viscosity increases with viscosity ratio λ.

Hydrodynamic interactions, i.e., correlations in the motions of particles mediated by flows in the embedding liquid are perhaps the key to explain the experimental observations. The collective dynamics of vesicles and rheology of semi-dilute and concentrated suspensions is an open question. The only experimental study of the hydrodynamic interaction of a pair of giant vesicles [117] showed a cross-flow displacement after the vesicles have passed each other, which gives rise to self-diffusion. However, a detailed and systematic study is still needed. Recent experiments in microgravity conditions have investigated the equilibrium distribution of a vesicle suspension in a Couette flow [118], where a steady distribution takes place under a balance between lift forces and the shear induced diffusion due to hydrodynamic interactions. These experiments show that they have a significant influence on the structure of the suspension even at rather low volume fractions and allow a measurement of effective diffusion coefficients.

5. Outlook

Vesicles and red blood cells in flow exhibit rich even surprising behavior. Despite active research, many open problems remain. Concerning an individual vesicle, outstanding issues are its dynamics in time-dependent flows, e.g. oscillatory shear, where chaotic behavior is expected [119,120] or the effect of multi-component membrane, where flow-induced lipid redistribution may give rise to novel features in the shape dynamics. Collective dynamics of vesicles is largely unexplored area. Recent simulation work has shown intriguing clustering phenomena in capillary flows [64]; at high hematocrit, three phases have been reported: parachute-shaped RBCs aligned in a single file,

disordered discocyte-shape, and zig–zag phase. Another topic is the coupling of electric and hydrodynamic fields: number of puzzling phenomena have been reported [121–123] but modeling efforts are at a very early stage [124,125].

In conclusion, the complex dynamics of vesicles and red blood cells fascinates physicists, engineers, biologists and mathematicians, and promises to be a fertile source of exciting questions for interdisciplinary research.

Acknowledgements

C. Misbah and T. Podgorski acknowledge financial support from CNES (Centre National D'Etudes Spatiales) and from ANR MOSICOB. Petia M. Vlahovska was supported by NSF CAREER award CBET-0846247.

References

[1] B. Alberts, A. Johnson, J. Lewis, M. Raff, K. Roberts, P. Walter, Molecular Biology of the Cell, 4th edition, Garland Publishing Inc., New York, 2002.
[2] R. Lipowsky, E. Sackmann, Structure and Dynamics of Membranes, Elsevier, Amsterdam, 1995.
[3] R. Lipowsky, The conformation of membranes, Nature 349 (1991) 475–481.
[4] P.R. Leduc, M.S. Wong, P.M. Ferreira, R.E. Groff, K. Haslinger, M.P. Koonce, W.Y. Lee, J.C. Love, J.A. McCammon, N.A. Monteiro-Riviere, V.M. Rotello, G.W. Rubloff, R. Westervelt, M. Yoda, Towards an in vivo biologically inspired nanofactory, Nat. Nanotechnol. 2 (2007) 3–7.
[5] V. Noireaux, A. Libchaber, A vesicle bioreactor as a step toward an artificial cell assembly, PNAS 101 (2004) 17669–17674.
[6] M. Karlsson, M. Davidson, R. Karlsson, A. Karlsson, J. Bergenholtz, Z. Konkoli, A. Jesorka, T. Lobovkina, J. Hurtig, M. Voinova, O. Orwar, Biomimetic nanoscale reactors and networks, Ann. Rev. Phys. Chem. 55 (2004) 613–649.
[7] T.M. Allen, P.R. Cullis, Drug delivery systems: Entering the mainstream, Science 303 (2004) 1818–1822.
[8] G. Gregoriadis, Engineering liposomes for drug delivery, Trends Biotechnol. 13 (1995) 527–537.
[9] D.R. Arifin, A.F. Palmer, Polymersome encapsulated hemoglobin: A novel type of oxygen carrier, Biomacromolecules 6 (2005) 2172–2181.
[10] R. Dimova, K.A. Riske, S. Aranda, N. Bezlyepkina, R.L. Knorr, R. Lipowsky, Giant vesicles in electric fields, Soft Matter 3 (2007) 817–827.
[11] R. Dimova, personal communication.
[12] M.-A. Mader, V. Vitkova, M. Abkarian, A. Viallat, T. Podgorski, Dynamics of viscous vesicles in shear flow, Eur. Phys. J. E 19 (2006) 389–397.
[13] W. Helfrich, Elastic properties of lipid bilayers – Theory and possible experiments, Z. Naturforsch. 28c (1973) 693–703.
[14] U. Seifert, Configurations of fluid membranes and vesicles, Adv. Phys. 46 (1997) 13–137.
[15] D. Barthes-Biesel, Role of interfacial properties on the motion and deformation of capsules in shear flow, Physica A 172 (1991) 103–124.
[16] C. Pozrikidis, Modeling and Simulation of Capsules and Biological Cells, CRC Press, 2003.
[17] M. Bloom, E. Evans, O.G. Mouritsen, Physical properties of the fluid lipid bilayer component of cell membranes – A perspective, Q. Rev. Biophys. 24 (1991) 293–397.
[18] R. Dimova, S. Aranda, N. Bezlyepkina, V. Nikolov, K.A. Riske, R. Lipowsky, A practical guide to giant vesicles: Probing the membrane nanoregime via optical microscopy, J. Phys. Condens. Matter 18 (2006) S1151–S1176.
[19] F.L. Brown, Elastic modeling of biomembranes and lipid bilayers, Annu. Rev. Phys. Chem. 59 (2008) 685–712.
[20] H. Dobereiner, Properties of giant vesicles, Curr. Opin. Colloid Interface Sci. 5 (2000) 256–263.
[21] D. Barthes-Biesel, Capsule motion is flow: Deformation and membrane buckling, C. R. Physique 10 (8) (2009) 764–774, this issue.
[22] E. Evans, R. Skalak, Mechanics and Thermodynamics of Biomembranes, CRC Press, Boca Raton, Florida, 1980.
[23] J.T. Jenkins, The equations of mechanical equilibrium of a model membrane, SIAM J. Appl. Math. 32 (1977) 755.
[24] M.M. Kozlov, Membrane shape equations, J. Phys. Condens. Matter 18 (2006) S1177–S1190.
[25] U. Seifert, Fluid membranes in hydrodynamic flow fields: Formalism and an application to fluctuating quasispherical vesicles, Eur. Phys. J. B 8 (1999) 405–415.
[26] U. Seifert, K. Berndl, R. Lipowsky, Shape transformations of vesicles: Phase diagram for spontaneous-curvature and bilayer-coupling models, Phys. Rev. A 44 (1991) 1182–1202.
[27] R. Blowers, E.M. Clarkson, M. Maizels, Flicker phenomenon in human erythrocytes, J. Physiol. 113 (1951) 228–239.
[28] F. Brochard, J.F. Lennon, Frequency spectrum of the flicker phenomenon in erythrocytes, J. Phys. (France) 36 (1975) 1035–1047.
[29] L. Miao, M.A. Lomholt, J. Kleis, Dynamics of shape fluctuations of quasi-spherical vesicles revisited, Eur. Phys. J. E 9 (2002) 143–160.
[30] L.G. Leal, Advanced Transport Phenomena, Cambridge University Press, 2007.
[31] K.H. de Haas, C. Blom, D. van den Ende, M.H.G. Duits, J. Mellema, Deformation of giant lipid bilayer vesicles in shear flow, Phys. Rev. E 56 (1997) 7132–7137.
[32] V. Kantsler, V. Steinberg, Orientation and dynamics of a vesicle in tank-treading motion in shear flow, Phys. Rev. Lett. 95 (2005) 258101.
[33] V. Kantsler, V. Steinberg, Transition to tumbling and two regimes of tumbling motion of a vesicle in shear flow, Phys. Rev. Lett. 96 (2006) 036001.
[34] M. Abkarian, A. Viallat, Vesicles and red blood cells in shear flow, Soft Matter 4 (2008) 653–657.
[35] J. Deschamps, V. Kantsler, V. Steinberg, Phase diagram of single vesicle dynamical states in shear flow, Phys. Rev. Lett. 102 (11) (2009) 118105.
[36] C. Misbah, Vacillating breathing and tumbling of vesicles under shear flow, Phys. Rev. Lett. 96 (2006) 028104.

[37] S.R. Keller, R. Skalak, Motion of a tank-reading ellipsoidal particle in shear flow, J. Fluid Mech. 120 (1982) 27–47.
[38] H. Noguchi, G. Gompper, Swinging and tumbling of fluid vesicles in shear flow, Phys. Rev. Lett. 98 (2007) 128103.
[39] P.M. Vlahovska, R. Gracia, Dynamics of a viscous vesicle in linear flows, Phys. Rev. E 75 (2007) 016313.
[40] M.-A. Mader, H. Ez-Zahraouy, C. Misbah, T. Podgorski, On coupling between the orientation and the shape of a vesicle under a shear flow, Eur. Phys. J. E 22 (2007) 275–280.
[41] G. Danker, T. Biben, T. Podgorski, C. Verdier, C. Misbah, Dynamics and rheology of a dilute suspension of vesicles: Higher order theory, Phys. Rev. E 76 (2007) 041905.
[42] V.V. Lebedev, K.S. Turitsyn, S.S. Vergeles, Nearly spherical vesicles in an external flow, New J. Phys. 10 (2008) 043044.
[43] B. Kaoui, A. Farutin, C. Misbah, Vesicles under simple shear flow: Elucidating the role of relevant control parameters, Phys. Rev. E, in press.
[44] A. Farutin, T. Biben, C. Misbah, New progress in analytical theory for vesicles under flow, preprint, 2009.
[45] T. Biben, C. Misbah, On quantitative and new qualitative features of vesicles under flow: A numerical study, preprint, 2009.
[46] P. Olla, The behavior of closed inextensible membranes in linear and quadratic shear flows, Physica A 278 (2000) 87–106.
[47] V.V. Lebedev, K.S. Turitsyn, S.S. Vergeles, Dynamics of nearly spherical vesicles in an external flow, Phys. Rev. Lett. 99 (2007) 218101.
[48] R. Finken, A. Lamura, U. Seifert, G. Gompper, Two-dimensional fluctuating vesicles in linear shear flow, Eur. Phys. J. E 25 (2008) 309–321.
[49] H. Noguchi, G. Gompper, Dynamics of fluid vesicles in shear flow: Effect of membrane viscosity and thermal fluctuations, Phys. Rev. E 72 (2005) 011901.
[50] N. Fa, C.M. Marques, E. Mendes, A.P. Schroder, Rheology of giant vesicles: A micropipette study, Phys. Rev. Lett. 92 (2004) 108103.
[51] V. Kantsler, E. Segre, V. Steinberg, Vesicle dynamics in time-dependent elongation flow: Wrinkling instability, Phys. Rev. Lett. 99 (2007) 178102.
[52] K.S. Turitsyn, S.S. Vergeles, Wrinkling of vesicles during transient dynamics in elongational flow, Phys. Rev. Lett. 100 (2008) 028103.
[53] H. Noguchi, Membrane simulation models from nanometer to micrometer scale, J. Phys. Soc. Japan 78 (2009) 041007.
[54] J.C. Shillcock, R. Lipowsky, The computational route from bilayer membranes to vesicle fusion, J. Phys. Condens. Matter 18 (2006) S1191–S1219.
[55] M. Muller, K. Katsov, M. Schick, Biological and synthetic membranes: What can be learned from a coarse-grained description? Phys. Rep. 434 (2006) 113–176.
[56] M. Kraus, W. Wintz, U. Seifert, R. Lipowsky, Fluid vesicle in shear flow, Phys. Rev. Lett. 77 (1996) 3685–3688.
[57] I. Cantat, C. Misbah, Lift force and dynamical unbinding of adhering vesicles under shear flow, Phys. Rev. Lett. 83 (1999) 880–883.
[58] B. Kaoui, G.H. Ristow, I. Cantat, C. Misbah, W. Zimmermann, Lateral migration of a two-dimensional vesicle in unbounded Poiseuille flow, Phys. Rev. E 77 (2008) 021903.
[59] S.K. Veerapaneni, D. Gueyffier, D. Zorin, G. Biros, A boundary integral method for simulating the dynamics of inextensible vesicles suspended in a viscous fluid in 2D, J. Comp. Phys. 228 (7) (2009) 2334–2353.
[60] K.A. Smith, W.E. Uspal, Shear-driven release of a bud from a multicomponent vesicle, J. Chem. Phys. 126 (2007) 075102.
[61] P.D. Richardson, I.V. Pivkin, G.E. Karniadakis, Red cells in shear flow: Dissipative particle dynamics modeling, Biorheology 45 (2008) 107–108.
[62] H. Noguchi, G. Gompper, Fluid vesicles with viscous membranes in shear flow, Phys. Rev. Lett. 93 (2004) 258102.
[63] H. Noguchi, G. Gompper, Shape transitions of fluid vesicles and red-blood cells in capillary flows, PNAS 102 (2005) 14159–14164.
[64] J.L. McWhirter, H. Noguchi, G. Gompper, Flow-induced clustering and alignment of vesicles and red blood cells in microcapillaries, PNAS 106 (15) (2009) 6039–6043.
[65] S. Messlinger, B. Schmidt, H. Noguchi, G. Gompper, Dynamical regimes and hydrodynamic lift of viscous vesicles under shear, Phys. Rev. E 80 (2009) 011901.
[66] T. Biben, C. Misbah, Tumbling of vesicles under shear flow within an advected-field approach, Phys. Rev. E 67 (2003) 031908.
[67] J. Beaucourt, F. Rioual, T. Seon, T. Biben, C. Misbah, Steady to unsteady dynamics of a vesicle in a flow, Phys. Rev. E 69 (2004) 011906.
[68] T. Biben, K. Kassner, C. Misbah, Phase-field approach to three-dimensional vesicle dynamics, Phys. Rev. E 72 (2005) 041921.
[69] Q. Du, C. Liu, X. Wang, Simulating the deformation of vesicle membranes under elastic bending energy in three dimensions, J. Comp. Phys. 212 (2006) 757–777.
[70] F. Feng, W.S. Klug, Finite element modeling of lipid bilayer membranes, J. Comp. Phys. 220 (2006) 394–408.
[71] L. Ma, W. Klug, Viscous regularization and r-adaptive remeshing for finite element analysis of lipid membrane mechanics, J. Comp. Phys. 227 (2008) 5816–5835.
[72] S. Chien, Red cell deformability and its relevance to blood flow, Annu. Rev. Physiol. 49 (1987) 177–192.
[73] C.D. Eggleton, A.S. Popel, Large deformation of red blood cell ghosts in a simple shear flow, Phys. Fluids 10 (1998) 1834–1845.
[74] P. Bagchi, Mesoscale simulation of blood flow in small vessels, Biophys. J. 92 (2007) 1858–1877.
[75] T.W. Secomb, R. Skalak, N. Ozkaya, J.F. Gross, Flow of axisymmetrical red blood cells in narrow capillaries, J. Fluid Mech. 163 (1986) 405–423.
[76] J.B. Freund, Leukocyte margination in a model microvessel, Phys. Fluids 19 (2007) 023301.
[77] C. Pozrikidis, Effect of membrane bending stiffness on the deformation of capsules in simple shear flow, J. Fluid Mech. 440 (2001) 269–291.
[78] M. Abkarian, M. Faivre, A. Viallat, Swinging of red blood cells under shear flow, Phys. Rev. Lett. 98 (2007) 188302.
[79] M. Bibtol, Red blood cell orientation in orbit $C = 0$, Biophys. J. 49 (1986) 1055–1068.
[80] A. Walter, H. Rehage, H. Leonhard, Shear induced deformation of microcapsules: Shape oscillations and membrane folding, Colloids Surf. A 183–185 (2001) 123–132.
[81] P. Erni, P. Fischer, E. Windhab, Deformation of single emulsion drops covered with a viscoelastic adsorbed protein layer in simple shear flow, Appl. Phys. Lett. 87 (2005) 244104.
[82] J.M. Skotheim, T.W. Secomb, Red blood cells and other nonspherical capsules in shear flow: Oscillatory dynamics and the tank-treading-to-tumbling transition, Phys. Rev. Lett. 98 (2007) 078301.

[83] S. Kessler, R. Finken, U. Seifert, Swinging and tumbling of elastic capsules in shear flow, J. Fluid Mech. 605 (2008) 207–226.
[84] Y. Sui, Y.T. Chew, P. Roy, Y.P. Cheng, H.T. Low, Dynamic motion of red blood cells in simple shear flow, Phys. Fluids 20 (2008) 112106.
[85] P. Bagchi, R.M. Kalluri, Dynamics of nonspherical capsules in shear flow, Phys. Rev. E 80 (2009) 016307.
[86] P.M. Vlahovska, G. Danker, C. Misbah, Swinging of drops enclosed by elastic membranes, in preparation.
[87] S. Guido, G. Tomaiuolo, Microconfined flow behavior of red blood cells in vitro, C. R. Physique 10 (8) (2009) 751–763, this issue.
[88] S.P. Sutera, R. Skalak, The history of Poiseuille's law, Annu. Rev. Fluid Mech. 25 (1993) 1–19.
[89] A.S. Popel, P.C. Johnson, Microcirculation and hemorheology, Annu. Rev. Fluid Mech. 37 (1) (2005) 43–69.
[90] F.P. Bretherton, The motion of rigid particles in a shear flow at low Reynolds number, J. Fluid Mech. 14 (1962) 284–304.
[91] L.G. Leal, Particle motions in a viscous fluid, Annu. Rev. Fluid Mech. 12 (1980) 435–476.
[92] B. Lorz, R. Simson, J. Nardi, E. Sakmann, Weakly adhering vesicles in shear flows: Tanktreading and anomalous lift force, Europhys. Lett. 51 (2000) 468–474.
[93] M. Abkarian, C. Lartigue, A. Viallat, Tank treading and unbinding of deformable vesicles in shear flow: Determination of the lift force, Phys. Rev. Lett. 88 (2002) 068103.
[94] M. Abkarian, A. Viallat, Dynamics of vesicles in a wall-bounded shear flow, Biophys. J. 89 (2005) 1055–1066.
[95] N. Callens, C. Minetti, G. Coupier, M.-A. Mader, F. Dubois, C. Misbah, T. Podgorski, Hydrodynamic lift of vesicles under shear flow in microgravity, Europhys. Lett. 83 (2008) 24002.
[96] I. Cantat, C. Misbah, Dynamics and similarity laws for adhering vesicles in haptotaxis, Phys. Rev. Lett. 83 (1999) 235–238.
[97] S. Sukumaran, U. Seifert, Influence of shear flow on vesicle near a wall: A numerical study, Phys. Rev. E 64 (2001) 011916.
[98] U. Seifert, Hydrodynamic lift on bound vesicles, Phys. Rev. Lett. 83 (1999) 876–879.
[99] P. Olla, The lift on a tank treading ellipsoidal cell in a shear flow, J. Phys. II France 7 (1997) 1533–1540.
[100] P. Olla, The role of tank-treading motions in the transverse migration of a spheroidal vesicle in a shear flow, J. Phys. A: Math. Gen. 30 (1997) 317–329.
[101] P. Olla, Simplified model for red cell dynamics in small blood vessels, Phys. Rev. Lett. 82 (1999) 453–456.
[102] S. Kim, S.J. Karrila, Microhydrodynamics: Principles and Selected Applications, Butterworth-Heinemann, 1991.
[103] R. Skalak, Science 164 (1969) 717.
[104] Y. Suzuki, N. Tateishi, M. Soutani, N. Maeda, Microcirculation 3 (1996) 49.
[105] T.W. Secomb, R. Skalak, Microvascular Research 24 (1982) 194.
[106] B. Kaoui, G. Biros, C. Misbah, Why do red blood cells move asymmetric even in a symmetric flow? Phys. Rev. Lett. 103 (2009) 188101.
[107] V. Vitkova, M. Mader, T. Podgorski, Deformation of vesicles flowing through capillaries, Europhys. Lett. 68 (2004) 398–404.
[108] R. Bruinsma, Rheology and shape transitions of vesicles under capillary flow, Physica A 234 (1996) 249–270.
[109] G. Danker, P.M. Vlahovska, C. Misbah, Vesicles in Poiseuille flow, Phys. Rev. Lett. 102 (2009) 148102.
[110] G. Coupier, B. Kaoui, T. Podgorski, C. Misbah, Noninertial lateral migration of vesicles in bounded Poiseuille flow, Phys. Fluids 20 (2009) 111702.
[111] P.C.-H. Chan, L.G. Leal, Motion of a deformable drop in a second-order fluid, J. Fluid Mech. 92 (1979) 131–170.
[112] M. Faivre, M. Abkarian, K. Bickraj, H.A. Stone, Geometrical focusing of cells in a microfluidic device: An approach to separate blood plasma, Biorheology 43 (2006) 147–159.
[113] C. Pozrikidis, Boundary Integral and Singularity Methods for Linearized Viscous Flow, Cambridge University Press, 1992.
[114] G. Danker, C. Misbah, Rheology of a dilute suspension of vesicles, Phys. Rev. Lett. 98 (2007) 088104.
[115] V. Vitkova, M. Mader, B. Polack, C. Misbah, T. Podgorski, Micro–macro link in rheology of erythrocyte and vesicle suspensions, Biophys. J. 95 (6) (2008) L33–L35.
[116] S.S. Vergeles, Rheological properties of a vesicle suspension, JETP 87 (2008) 511–515.
[117] V. Kantsler, E. Segre, V. Steinberg, Dynamics of interacting vesicles and rheology of vesicle suspension in shear flow, Europhys. Lett. 82 (2008) 58005.
[118] T. Podgorski, N. Callens, C. Minetti, G. Coupier, F. Dubois, C. Misbah, Biomics experiment: Structure and dynamics of a vesicle suspension in a shear flow, in: Proceedings of the 19th ESA-PAC Symposium on Rocket and Balloon Programmes and Related Research, 2009, pp. 1–6.
[119] S. Kessler, R. Finken, U. Seifert, Elastic capsules in shear flow: Analytical solutions for constant and time-dependent shear rates, Eur. Phys. J. E 29 (2009) 399–413.
[120] Y.-N. Young, J. Bławzdziewicz, V. Cristini, R.H. Goodman, Hysteretic and chaotic dynamics of viscous drops in creeping flows with rotation, J. Fluid Mech. 607 (2008) 209–234.
[121] R. Dimova, N. Bezlyepkina, M.D. Jordo, R.L. Knorr, K.A. Riske, M. Staykova, P.M. Vlahovska, T. Yamamoto, P. Yang, R. Lipowsky, Vesicles in electric fields: Some novel aspects of membrane behavior, Soft Matter (2009), in press, doi:10.1039/B901963D.
[122] M. Staykova, R. Lipowsky, R. Dimova, Membrane flow patterns in multicomponent giant vesicles induced by alternating electric fields, Soft Matter 4 (2008) 2168–2171.
[123] S. Lecuyer, W.D. Ristenpart, O. Vincent, H.A. Stone, Electrohydrodynamic size stratification and flow separation of giant vesicles, Appl. Phys. Lett. 92 (2008) 104105.
[124] D. Lacoste, G.I. Menon, M.Z. Bazant, J.F. Joanny, Electrostatic and electrokinetic contributions to the elastic moduli of a driven membrane, EPJE 28 (2009) 243–264.
[125] P.M. Vlahovska, R.S. Gracia, S. Aranda-Espinoza, R. Dimova, Electrohydrodynamic model of vesicle deformation in alternating electric fields, Biophys. J. 96 (2009) 4789–4803.